A comparison of ceramic and carbon-based reductants for vitrification of low-activity waste

RIGBY, Jessica, MILLER, Megan G., DAVIDSON, Stephen, BOHRMANN, Natalie C., MARCIAL, José, SEO, Ji-Hye, SCRIMSHIRE, Alex <http://orcid.org/0000-0002-6828-3620>, BINGHAM, Paul <http://orcid.org/0000-0001-6017-0798>, HALL, Mark A., EATON, Will C. and KRUGER, Albert A.

Received: 26 June 2025 | Revised: 29 August 2025 | Accepted: 12 September 2025

DOI: 10.1111/ijag.70009

INTERNATIONAL JOURNAL OF Applied Glass SCIENCE

RESEARCH ARTICLE

A comparison of ceramic and carbon-based reductants for vitrification of low-activity waste

Jessica Rigby[1] | **Megan G. Miller**[1] | **Stephen Davidson**[1] | **Natalie C. Bohrmann**[1] | **José Marcial**[1] | **Ji-Hye Seo**[1] | **Alex Scrimshire**[2] | **Paul A. Bingham**[2] | **Mark A. Hall**[1] | **Will C. Eaton**[1] | **Albert A. Kruger**[3]

[1]Pacific Northwest National Laboratory, Richland, Washington, USA

[2]Materials and Engineering Research Institute, College of Business, Technology and Engineering, Sheffield Hallam University, Sheffield, UK

[3]U.S. Department of Energy, Hanford Field Office, Richland, Washington, USA

Correspondence
Jessica Rigby, Pacific Northwest National Laboratory, Richland, WA 99354, USA.
Email: jessica.rigby@pnnl.gov

Initial foaming results and gas evolution for these alternative ceramic reductants were presented at the Glass and Optical Materials Division of the American Ceramic Society in Las Vegas, USA, 2024 and in Vancouver, BC, 2025.

Funding information
Pacific Northwest National Laboratory is operated by Battelle for DOE, Grant/Award Number: DE-SAC05-76RL01830

Abstract

Sucrose is the current baseline additive at the Hanford Waste Treatment and Immobilization Plant in Washington to control foaming during waste feed to glass transitions and the redox state of the glass melt. Alternative reductants are being investigated to alleviate strain on effluent treatment from toxic acetonitrile production from incomplete combustion of sucrose. This study evaluates ceramic additive options including B_4C, B_6Si, SiC, and VB_2 in simulated low-activity waste feed, as well as coke dust, probing the feed volume expansion during melting as well as the gas evolution. All alternative reductant options examined significantly reduced acetonitrile production; however, there was variability in their effectiveness as foam-reducing agents. VB_2 and coke matched the performance of sucrose in controlling foam volume and glass redox state, but with notably less acetonitrile production. B_4C, B_6Si, and SiC demonstrated improved foam control and very little acetonitrile production; however, the final glasses were over-reduced, that is, $Fe^{2+}/Fe_T \geq 0.5$. These alternative reductant studies provide operational flexibility to the operation of the vitrification plant, as well as options for alternative raw materials in industrial glass melting.

KEYWORDS
alternate reductants, off-gas, radioactive waste, redox, vitrification

1 | INTRODUCTION

There are over 200,000 m^3 of nuclear waste, historically stored in 177 carbon-steel underground tanks at the Hanford site in Washington State. The Waste Treatment & Immobilization Plant (WTP) was built to vitrify the radioactive waste for long-term immobilization of the radionuclides.[1–3] Low-activity waste (LAW), making up ~90% of the waste inventory by volume, is to be vitrified in the LAW Vitrification Facility post filtration and cesium ion exchange in Tank Side Cesium Removal.[1,2,4,5] High-level waste (HLW) is to be processed in a separate HLW vitrification facility on the Hanford site.[1] In both LAW and HLW vitrification facilities, waste will be mixed with

glass-forming chemicals and fed into the melter through a feed tube, landing on top of a pool of molten glass at ~1150°C.[1,6–14]

During the conversion of nuclear waste to glass, melting reactions form a reaction later called the "cold cap", which covers ~95% of the surface of the molten glass. Primary foam appears at the feed-melt interface when an early glass-forming melt closes open pores. Primary foam is a bulk foam,[7] which collapses internally as the volume of gas from residual conversion reactions expands as a function of increasing temperature. The increasing temperature also decreases the viscosity and surface tension of the transient glass-forming melt until the point at which the foam is no longer stable and the glass-forming melt can drain from bubble walls.[8,13] Coalescing bubbles and large gas-filled cavities eventually escape to the atmosphere at the cold-cap edges or vent holes. The cold cap and feed-to-glass reactions are the subject of many studies aiming to control foaming, improve melting rate, and mitigate volatilization of semi-volatile waste species.[14–18]

In general, the LAW feeds are nitrate rich and experience primary foaming in the 600–800°C temperature range, where the main contributing gas species are CO_x and NO_x. Secondary foaming can occur at higher temperatures after the collapse of primary foam, with the redox-dependent release of O_2 and SO_2 gasses above ~900°C.[14–15,19] Acetonitrile (CH_3CN) is a toxic substance that evolves from the incomplete combustion of sucrose, the baseline reductant for melter feeds.[20,21] Reduction of acetonitrile has been the subject of recent studies to reduce load on the current effluent treatment facility (ETF).[21] Organic carbon-based reductants have been explored for waste vitrification.[17,22–24] Formic acid has been shown to be less effective than sucrose in a high-iron high-level waste[17] as well as posing higher risks of melter flammability.[23,24] Graphite and coke dust were shown to be more effective in reducing foaming in the high-iron high-level waste feed; however, there are concerns with overreduction of the melt, particularly for graphite.[17] Neither of those compounds have been shown or are expected to produce acetonitrile.[17]

To obviate flammability and toxic off gas concerns, Pacific Northwest National Laboratory (PNNL) recently proposed boron nitride (BN) as an alternative ceramic reductant,[25] demonstrating the crucible scale to be more effective than sucrose in reducing foam volume during melting. BN as an additive showed 90% reduction of acetonitrile and effective redox control in the final glass product. Crucially, the study highlighted that the mechanism of foaming can be controlled by adjusting the glass-forming chemicals. By introducing these components as thermally stable ceramic compounds, they only decompose and interact with the melt at elevated temperatures. This approach differs from the manipulation of the evolving gases by the addition of organics at lower temperatures.[25] The study paves the way for the exploration of other ceramic systems that could exploit the same mechanism.

TABLE 1 Thermal decomposition temperature in inert atmosphere of the reductant additives explored in simulated Tank 241-AP-106 (hereafter called AP-106) and others for comparison.

Compound	Decomposition temperature (°C)	Notes
$C_{12}H_{22}O_{11}$	~186	Decomposes[33,34]
BN	~2973	Sublimes[35,36]
SiC	~2730	Decomposes incongruently[36,37]
B_4C	~2450	Melts[36,38]
B_6Si	~1850–2300	Sparse data[36,39,40]
VB_2	~2980	1126°C onset of oxidation in air[36,41]
C (Coke dust)	~500–1000	Composition dependent[42,43]
C (Graphite)	>400	Oxidation in air[36,44]

The following study aimed to compare a further range of additives that include proportions of glass-forming chemicals to study their effects on foaming, gas evolution, and final glass redox. Two directions were taken in this study, the first explored coke dust as an additive that has been long used in the glass industry,[26–29] and recycling coke from coal carbonization is a growing field of research. Coke and related waste products are used in steelworks, adsorbent materials, and geopolymers.[30–32] Coke is known to be stable up to high temperatures and influence secondary foam behavior.[17,29] The second was exploring alternative refractory-like ceramics following from the study conducted at PNNL,[25] which showed successful foam reduction using BN as discussed earlier. Boron carbide (B_4C), boron silicide (B_6Si), silicon carbide (SiC), and vanadium diboride (VB_2) all contain glass forming species and were explored. The thermal decomposition for each of these species in inert atmospheres, unless otherwise stated are given in Table 1. The thermal condition of a glass melt will alter the temperature of decomposition of compounds, while the sample in this study will all be heated in air and the oxygen availability will be dependent on the redox state of the feed and glass melt during heating. Without detailed studies of these compounds in glass melts, the table provides a point of comparison for the data collected throughout this work.

TABLE 2 Nominal waste composition of the AP-106 simulated waste feed.

Chemical source	Target (g/L waste)
Re solution	11.03
KI	0.1784
$Al(NO_3)3{\cdot}9H_2O$	115.70
$Ca(NO_3)_2{\cdot}9H_2O$	0.0829
$Fe(NO_3)_3{\cdot}9H_2O$	0.0807
H_3BO_3	0.1455
$Ni(OH)_2$	0.0287
SiO_2	0.1204
Na_2CrO_4	1.30
KOH	4.65
NaOH	130.58
NaCl	3.88
$Na_3PO_4{\cdot}12H_2O$	6.70
Na_2SO_4	6.40
$NaNO_2$	73.35
$NaNO_3$	57.46
$NaC_2H_3O_2$ (sodium acetate)	6.83
$NaHCO_2$ (sodium formate)	5.72
$Na_2C_2O_4$ (sodium oxalate)	5.25
Na_2CO_3	9.54

2 | MATERIALS AND METHODS

2.1 | Simulant preparation

The composition used in this study was based on the composition expected in the Tank 241-AP-106 (hereafter called AP-106) tank, which is the current interim LAW storage tank.[1,5,45] Currently, the AP-106 tank holds waste that was previously in the Tank 241-AP-107 (hereafter called AP-107), and reported as AP-107 previously[5,25,46,47] diluted with water and NaOH.[5] The previous study on BN as an alternative reductant[25] was performed on the composition of the original AP-107 tank waste, therefore the sucrose and BN additions have been replicated in this study with the current composition for consistency. AP-106 simulant, composition shown in Table 2, was batched on a 2-decimal point balance for target weights ≥1 g and on a 4-decimal point scale for target weights <1 g, using raw materials with > 98% purity. Chemicals were mixed in water to a final volume of 1 L.

2.2 | Melter feed additives

Coke dust was provided by Phillips 66 in two forms, green and calcined coke. Green coke was retrieved directly as a by-product of petroleum production, and calcining coke involves heating the coke to remove volatile components. Samples of powdered green and calcined coke were mounted using carbon tape onto a sample holder and then sputter coated with a 2-nm conductive iridium coating. Scanning electron microscopy–energy dispersive spectroscopy (SEM–EDS) was measured using a JEOL 7001F SEM operated at 15 kV and 13 nA. Compositional mapping and compositional measurements were taken using a Bruker Flash 6 60 EDS detector.

When B_6Si, SiC, VB_2, and B_4C were added, Si and/or B were reduced pro rata from the quantities of SiO_2 or H_3BO_3 added as glass forming chemicals. No vanadium-containing species is present in the batch compositions, so the final glasses made with VB_2 will contain V likely in the oxide form V_2O_5. V_2O_5 may impact the properties of the final glass. The impact of the oxidation from VB_2 to V_2O_5 and B_2O_3 on the Fe redox state when melted in air is within the scope of this study, but further assessment of the glass properties should be performed to ensure the glass product quality remains suitable for long-term disposal. Both coke samples were compared as reductants in the current study at C/N = 0.75, equivalent to sucrose. The quantities were added based on a molar ratio of X to nitrates in the feed, either C/N (SiC, B_4C), Si/N (B_6Si), or V/N (VB_2) = 0.25. AP-106 melter feeds BN at BN/N = 0.25 and 0.75 were also generated for comparison with the previous BN study where the data were valuable, and the full characterization of this feed is given in Supporting Information S1.[25]

The reductants, as seen in Table 3, were added to the slurries during mixing to ensure homogeneity. Final melter feed slurry was either pumped into smaller containers for density, rheology, and loss-on drying measurements, or dried out at 105°C for 24 h. Dried slurry was then milled in a tungsten carbide vibratory mill for 2 min for further tests outlined in the following sections.

2.3 | Feed volume expansion testing

Pellets of 13 mm diameter were pressed using 0.9 g of each dried feed at ~10 MPa pressure. Pellets were then heated in a furnace at 10°C/min until the sample had fully melted and was flat. Images were captured on a camera through a viewport in the furnace every 5 s, and the area of the projected image was recorded. By assuming the rotational symmetry around a vertical axis and a glass density ~2.5 g cm^{-3}, volume can be calculated as described in Rigby et al.[25] and Marcial et al.[48] The average volumes of at least two runs were taken for each feed composition.

TABLE 3 Nominal composition of the AP-106 glass-forming chemicals (GFCs) for each variation in alternative reductant content.

G	AP-106 Sucrose	AP-106 Coke	AP-106 Coke	AP-106 B_4C	AP-106 SiC	AP-106 B_6Si (Si/N)	AP-106 VB_2 (V/N)
C/N	0.75	0.75	0.25	0.25	0.25	0.25	0.25
	Target (g/L feed)						
$AlSiO_5$ (kyanite)	65.68	65.68	66.89	66.89	66.89	66.89	66.89
H_3BO_3 (boric acid)	160.14	160.14	163.08	132.17	163.08	132.17	132.17
$CaSiO_3$ (wollastonite)	54.67	54.67	55.68	55.68	55.68	55.68	55.68
Fe_2O_3 (hematite)	47.24	47.24	48.11	48.11	48.11	48.11	48.11
$MgSiO_4$ (olivine)	26.78	26.78	27.28	27.28	27.28	27.28	27.28
SiO_2 (silica)	336.97	336.97	343.15	343.15	313.12	279.72	343.15
TiO_2 (rutile)	12.25	12.25	12.47	12.47	12.47	12.47	12.47
ZnO (zinc oxide)	31.68	31.68	32.27	32.27	32.27	32.27	32.27
$ZrSiO_4$ (zircon)	40.50	40.50	41.24	41.24	41.24	41.24	41.24
$C_{12}H_{22}O_{11}$ (Sucrose)	51.41						
Green coke		23.27	6.34				
Calcined coke		23.27					
B_4C				27.12			
SiC					19.68		
B_6Si						35.02	
VB_2							35.62

2.4 | Evolved gas analysis

Using a Hiden Analytical HPR R&D20 evolved gas analysis (EGA), the release rate of evolved gases was measured on ~1 g of each feed sample loaded into a silica tube inside a furnace. The furnace was heated to 1150°C at 10°C/min under argon flowing at 50 mL/min. The m/z signal intensities that were measured were normalized to the carrier gas intensity and converted to values recorded in parts per million (ppm). Background measurements were recorded for ~5 min before starting the furnace to subtract background gases from the final data.

2.5 | Glass redox analysis

^{57}Fe Mössbauer spectroscopy was used to investigate the form of Fe in the final glass samples. Powdered samples were diluted with graphite and placed into a room temperature ^{57}Fe Mössbauer spectrometer with a 25 mCi ^{57}Co source in a Rh matrix. The 14.4 keV γ-rays were produced by the decay of the source, and the source was driven with a constant acceleration by a SeeCo W304 drive unit. The γ-rays were detected using a SeeCo 45431 Kr proportional counter with a 1.745 kV bias voltage applied to the cathode. Transmission spectra of photons through the sample were recorded over a velocity range of ± 12 mm s^{-1} and calibrated with respect to α-Fe. Pseudo-Voight doublets were fitted to the spectra using Recoil software.

TABLE 4 Composition of coke sources by scanning electron microscopy–energy dispersive spectroscopy (SEM–EDS).

Element	Composition wt%[a] Green coke (GC)	Calcined coke (CC)
Carbon	94	90
Oxygen	5	8
Sulfur	0.5	0.4
Silicon	0.3	0.3
Calcium	0.1	0
Sodium	0.03	0.1
Iron	0.01	0.05
Aluminum	0	0.3

[a]Composition by SEM–EDS excludes elements lighter than C, including Li and B.

3 | RESULTS AND DISCUSSION

3.1 | The effect of coke addition on melting behavior

SEM–EDS mapping of the two coke sources in Figure 1 shows impurities semi-quantitatively listed in Table 4. These impurities are all components of the simulant or

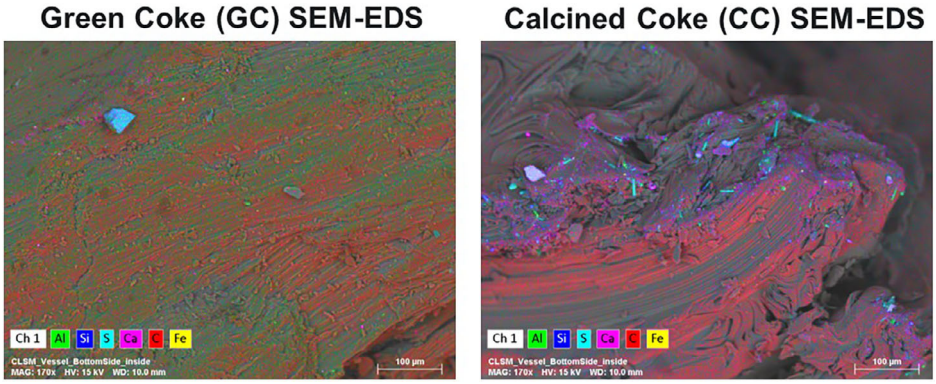

FIGURE 1 Scanning electron microscopy–energy dispersive spectroscopy (SEM–EDS) maps of green coke (left) and calcined coke (right) samples.

FIGURE 2 Image of green coke particles floating on the surface of feed.

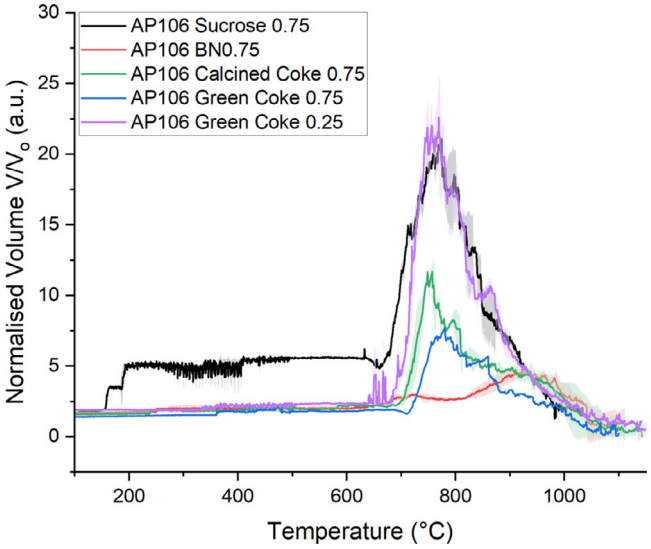

FIGURE 3 Feed volume expansion curves of AP-106 with green and calcined coke as reductants compared with boron nitride (BN) and sucrose at X/N ratios of 0.75, as well as green coke at 0.25, where X is "C" in sucrose and coke or "BN".

melter feed chemicals. SEM–EDS does not capture elements lighter than C, or some organic species more likely to be in the green coke based on the lack of processing, but for the elements available results suggest there is not a large difference in the purities of the green coke compared to the more processed calcined coke. Figure 2 shows some green coke dust floating on top of the melter feed slurry once mixed and left to settle; this behavior was observed in the previous study with BN powder floating to the top of the melter feed when left unagitated.[25]

A comparison of the feed volume expansion during melting is shown in Figure 3 for the baseline sucrose AP-106 feed (C/N = 0.75), AP-106 with BN (BN/N = 0.75), AP-106 batched with green coke (C/N = 0.25 and at C/N = 0.75), and batched with calcined coke (C/N = 0.75). The AP-106 baseline sucrose had a low-temperature foaming behavior caused by what appears to be a single large bubble at ~200°C continuing up to ~650°C where the main foaming took over. This occurred in both repetitions of the feed volume expansion tests with sucrose, and example images for one of the tests showing the single bubble beneath the main pellet are shown in Figure 4. This low-temperature foam event was not observed in the AP-107 baseline[25] and therefore must be a consequence of the minor compositional changes. The low-temperature foam from these experiments might not be an issue in large melter systems as the plenum temperature is likely to be upwards of 400°C;[49] however, this result should prompt further melter testing of the AP-106 composition prior to hot start-up with the baseline composition.

Both green and calcined coke additives at C/N = 0.75 are more effective in foam reduction across the melting temperature range compared to sucrose and neither showed low-temperature foaming events. Green coke at C/N = 0.25

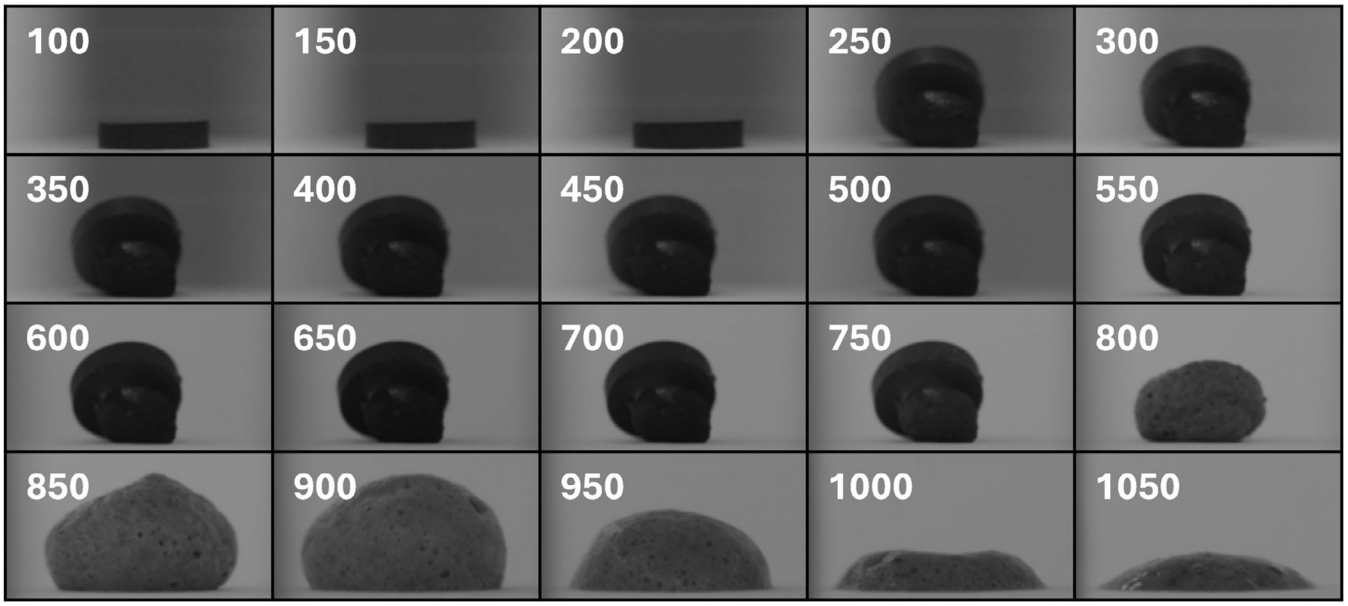

FIGURE 4 Images of AP-106 pellet with sucrose as a reductant during feed expansion testing showing large bubbles at low temperatures, growth of the primary foam, and then collapse into a glass melt.

had a similar volume profile as the baseline for the primary foam peak, but without low-temperature foaming. Given that there does not appear to be an advantage in foaming or impurities to using calcined coke that involves more costly processing, the remainder of this study is performed on green coke, and from this point forward referred to as "coke." BN remains more effective in suppressing foam volume during melting, following a very similar shaped curve to the previous AP-107 feed experiment.[25]

Low-temperature foaming in the AP-106 baseline with sucrose appears to be caused by the evolution of CO_2, N_2, and NO beginning at ~200°C, shown in the top graph in Figure 5. A similar gas profile is also seen in the coke sample at C/N = 0.25, albeit with a significant reduction in the evolution of CO_2. The consequence is that an increased low-temperature foam volume must be caused by the viscosity of the glass-forming/molten salt phase at the low temperature, that is, these gases are free to escape through open porosity in the coke sample but trapped in a large/multiple large bubbles within the sucrose sample. Overall, the gas quantities for the feed with coke at C/N 0.25 are much lower than the feed with sucrose. Coke at C/N = 0.75 has a rapid release of gas just above 400°C, which must escape through open porosity as there is no indication of this release in the foaming curve. After this release, there is a relatively small quantity of further gas release, resulting in lower foam volume than the other coke feeds. This rapid release of gas could be a reaction with organics in the coke, or the carbon itself reacting exothermally with the molten salt phase. It is likely to be undesirable for melter systems to have such a rapid release of gas that could add excess load to the off-gas system.

Based on the similarity in the main foam volume expansion peak, coke and sucrose do not have equivalent effects on foaming when equated for carbon molarity. Instead, it is sensible to assume coke is approximately three times more effective, that is, coke at C/N = 0.25 is as effective in reducing foam volume as sucrose at C/N = 0.75. In the previous BN study, a similar conclusion was drawn for BN/N ratios in the melter feed based on both foaming and final glass redox.[25] For this reason, the remainder of the study compares alternative reducing additives at X/N = 0.25, where X is either C, Si, or V to sucrose at C/N = 0.75.

3.2 | The effect of ceramic reductants on melting behavior

In previous work, it has been shown that graphite, which is thermally stable in air up to 3600°C,[36,44] begins to decompose in a simulated HLW glass melt between 1000 and 1100°C.[17] The hypothesis that BN as well as other refractory-like ceramics may reduce foam volume considerably by the mechanism of high-temperature release of glass forming species is further complicated by the results shown in Figure 6. There is notable foam reduction when the melter feed is batched with SiC, B_4C, and B_6Si, but addition of VB_2 has a comparable foam profile with temperature to the baseline sucrose feed between 600 and 1000°C.

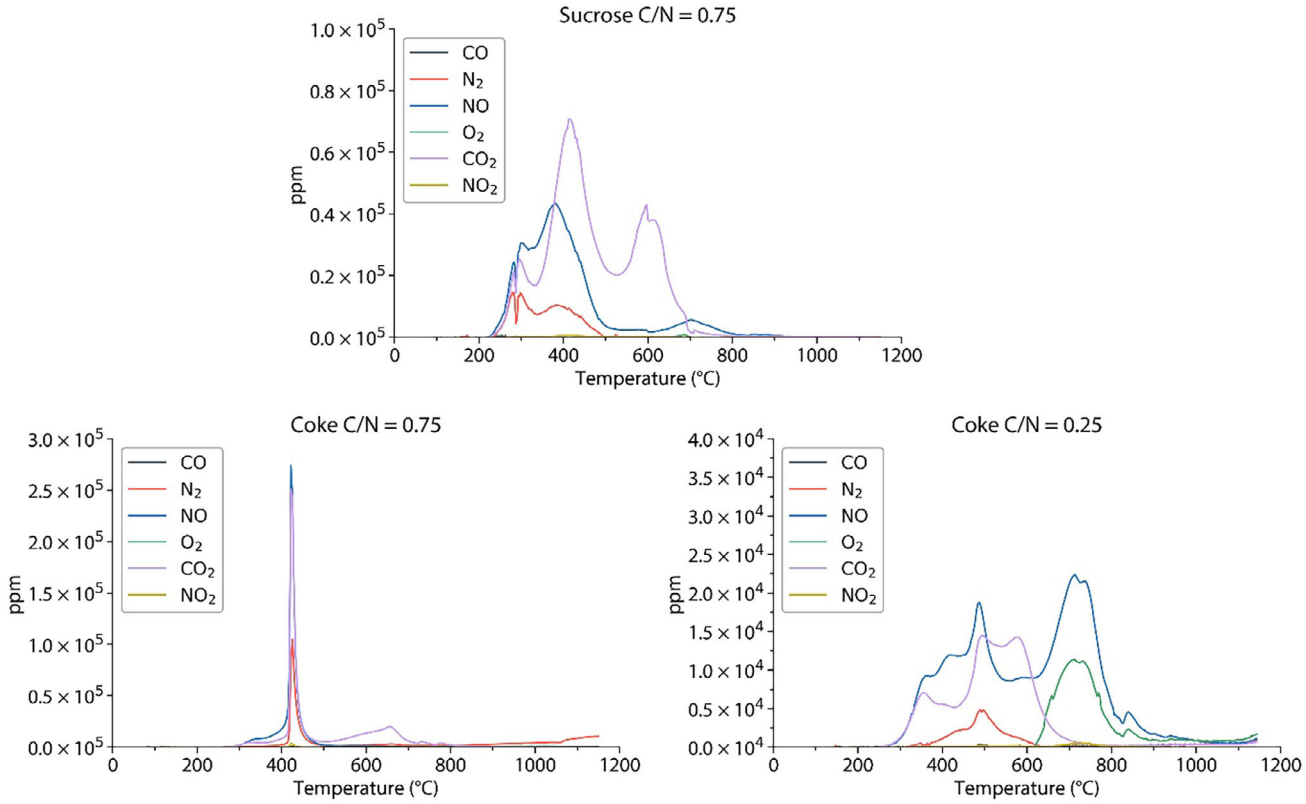

FIGURE 5 Evolved gases in the AP-106 feed with sucrose as a reductant (top), coke as a reductant C/N = 0.75 (bottom left) and C/N = 0.25 (bottom right).

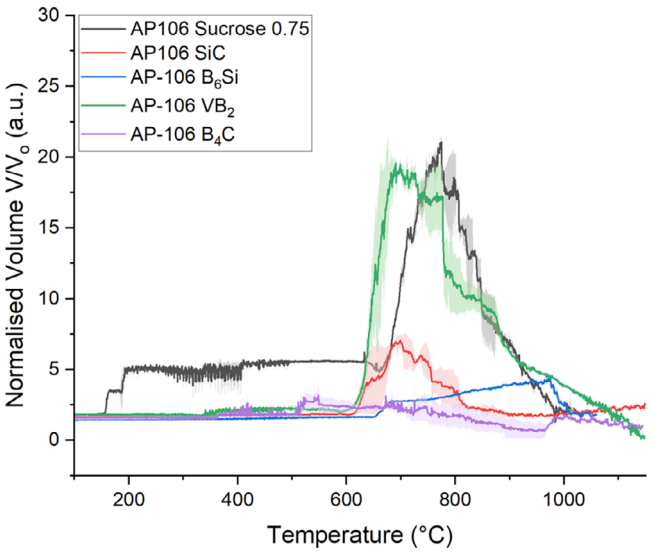

FIGURE 6 Feed volume expansion curves of AP-106 feed with SiC, B_6Si, VB_2, and B_4C as reductants at X/N ratios of 0.25, where X = C in SiC, Si in B_6Si, V in VB_2, and C in B_4C, compared with sucrose at C/N = 0.25.

Foaming in the feed with SiC resembles the shape of curves previously formed in HLW studies, showing similar total foam expansion volumes, but shifted to lower temperatures.[17,49] The collapse of the SiC foam by 800°C could be beneficial for processing, since primary foaming can readily collapse while the melt is not too viscous. Higher temperature foams persist when the melt viscosity has increased and is less readily collapsible. Bubblers in full-scale melters may make the higher temperature foaming less of an issue in a full-scale melter.[39–51] The B_6Si feed is a unique example of foam behavior that steadily increases until high temperature and then collapses around 1000°C. Further testing would be required to determine whether this is suitable for processing in a melter. There is very little foaming in the feed with B_4C comparable to the maximum BN feed (BN/N = 1.75) in previous work.[25]

Gas evolution profiles during melting for the refractory-like ceramic samples are shown in Figure 7. Main evolution of NO is apparent ~600°C in the SiC feed, overlapping with CO_2 evolution, as observed in the coke feed at C/N = 0.25 in Figure 5. This gas profile is what we would expect without manipulation of the nitrates with low-temperature organics and the behavior has been observed before in the gas evolution of the AP-107 feed without any reducing agents added.[25] In the sucrose feed, however, that NO is released at lower temperatures due to the sucrose reactions.[25] In the B_6Si feed (Figure 7), there is partial organic reaction with nitrates, while the secondary NO peak from thermal decomposition of nitrates above

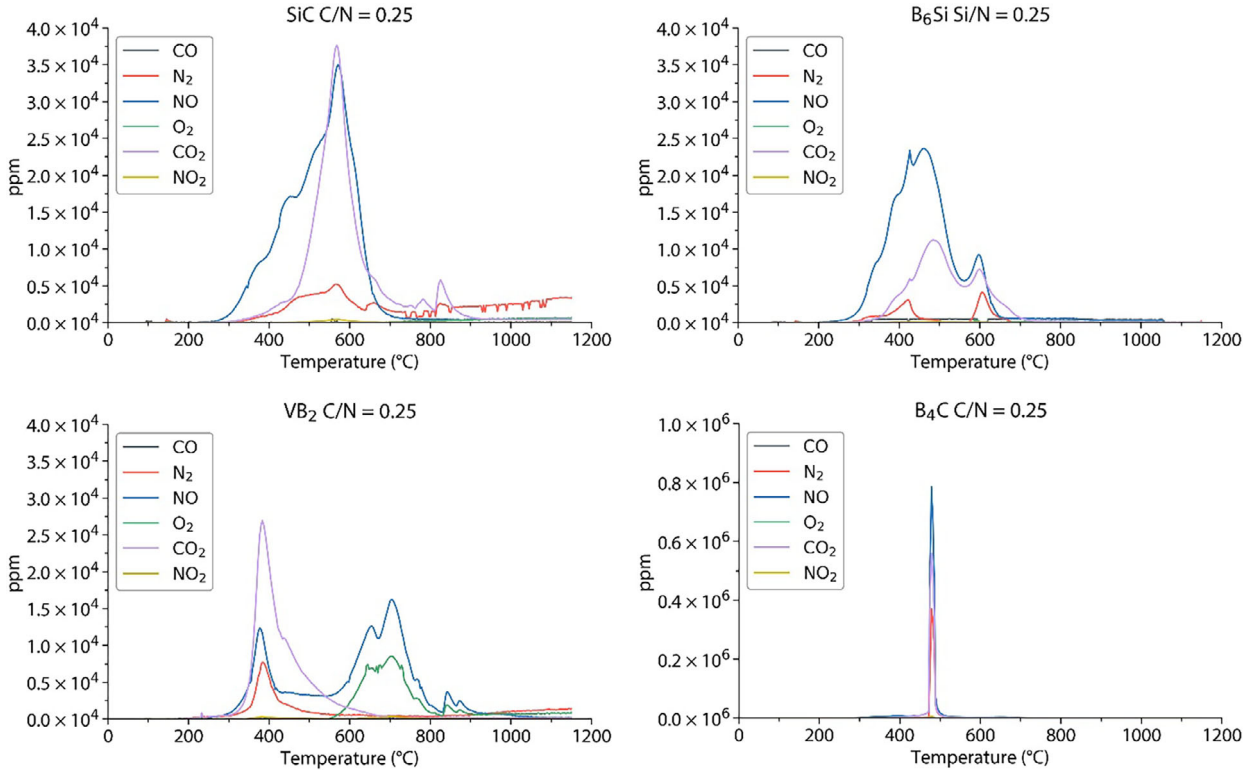

FIGURE 7 Major evolved gases in the AP-106 feed with SiC (top left), B_6Si (top right), VB_2 (bottom left), and B_4C (bottom right) as reductants.

600°C is significantly reduced compared to SiC. Both VB_2 and B_4C show at least partial reactions with nitrates below 400°C, but the main NO evolution comes after 600°C in VB_2 and in the rapid evolution of gases at 450°C in B_4C. It is postulated that there are organic impurities in the reductants that drive the partial NO evolution to occur at a lower temperature when the reductants are added.

A rapid release of NO, CO_2, and N_2 occurs in the feed with B_4C (Figure 7), similarly to the coke at 0.75 (Figure 5). This rapid evolution of large amounts of gases occurs at a temperature range that is usually associated with open porosity, before viscous glass melt formation.[52] The rapid release of gas aligns with a small but distinct increase in foam volume in the feed volume expansion curve (Figure 6). As discussed, for coke, this may not be desirable for either scaled-up melter testing or full-scale WTP operation.

3.3 | Evolution of semi-volatile species

The initial motivation to explore alternate reductants was to reduce acetonitrile off gas from the melter feeds. In Figure 8, all alternative reductants have significantly reduced the release of acetonitrile compared to the baseline reductant, sucrose, which is expected due to the lack of organics. However, what is interesting is the temperature at which the acetonitrile evolution peaks in the samples varies with each alternative reductant. The higher temperature and broad evolution of acetonitrile release in the SiC sample suggest it may follow the foaming curve, in that some of it is trapped within the primary foam and then released during foam collapse. It is comparable to the secondary peak of the acetonitrile in sucrose. The other reductants have acetonitrile peaks below the onset of primary foaming, and they are well-defined peaks as seen in the previous BN work.[25] B_6Si has the highest acetonitrile peak, this result aligns with the theory posed in the main gas evolution (Section 3.2) that the feed is higher in organic species. The impact of the increased organics is both a shifted the NO peak to lower temperatures and increased the acetonitrile evolution.

Sulfur retention is heavily studied for waste vitrification.[53] Release of SO_2 gas is an indication that less SO_3 is retained in the melt. The retention of sulfur in a glass melt is dependent on the solubility limit of the glass composition and redox state of the melt.[54] Previous work on AP-107 melter feed showed that both the quantity and temperature of evolution of SO_2 were influenced by the quantity of the reductant, or, consequently, the melt redox state. The SO_2 evolution for BN added at 0.25 ratio to AP-106 melter feed is compared with the other reductants in Figure 8. The temperature of evolution is comparable to that in AP-107.[25] There is no significant SO_2 evolution

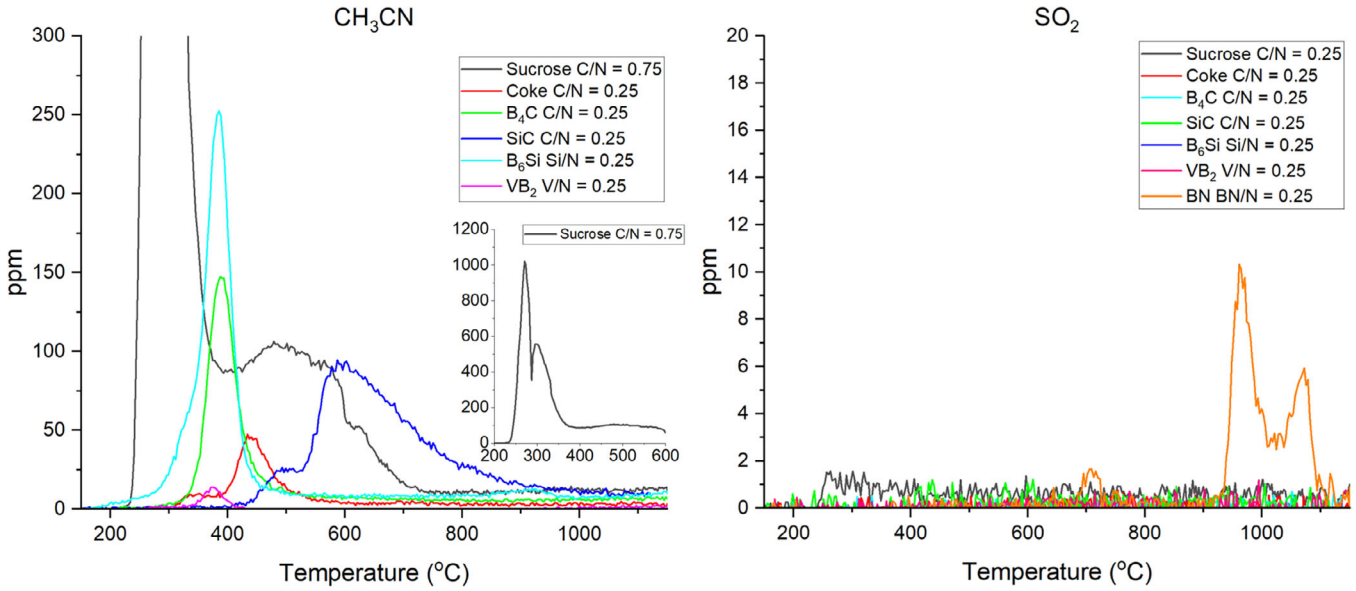

FIGURE 8 Minor gases evolved during melting the AP-106 feed with sucrose compared to alternative reductants. Acetonitrile production (left) inset shows the full scale of AP-106 feed with sucrose. SO_2 production (right) shows only evolution of SO_2 above the noise from AP-106 with boron nitride (BN) measured previously.

TABLE 5 Hyperfine splitting parameters from pseudo-Voight fits of ^{57}Fe Mössbauer spectra. Centre shift (CS) relative to α-Fe, ±0.02 mm s^{-1}. Relative area of each iron site ±2%.

Sample	Site	CS (mm s^{-1})	QS (mm s^{-1})	Relative area (%)
AP-106	Fe^{3+}	0.25	0.97	100
AP-106-Coke	Fe^{3+}	0.25	1	100
AP-106-B_4C	Fe^{3+}	0.31	0.79	50.5
	Fe^{2+}	0.93	2	49.5
AP-106-B_6Si	Fe^{3+}	0.42	0.85	27.7
	Fe^{2+}	0.98	1.96	72.3
AP-106-SiC	Fe^{3+}	0.33	0.83	65.0
	Fe^{2+}	0.92	2.05	35.0
AP-106-VB_2	Fe^{3+}	0.25	0.97	100

over the complete temperature range of melting for any of the additional reductants explored in this work. A full compositional analysis of the glass would need to be performed to confirm that all SO_3 is retained in the glass.

3.4 | Iron redox

Figure 9 shows the results of a hyperfine fitting of the pseudo-Voight functions fitted to the ^{57}Fe Mössbauer data of each melter feed melted at 1150°C and quenched. Iron redox state, in Table 5, was determined by the ratio of peak areas corresponding to Fe^{3+} and Fe^{2+} sites, assuming a recoil-free fraction ratio of $f(Fe^{3+}/Fe^{2+}) = 1.0$. The pseudo-Voight functions assign one doublet to each oxidation state in the glass but do not have the granularity to distinguish between coordination states of iron in each redox state, just an average coordination state. Within the approximate limit of detection of this method with the velocity range measured, we can be confident that no more than 10% of the Fe is in an Fe^{2+} redox state for the melter feeds with sucrose, coke, and VB_2 as reductant additives. This is assuming the ranges for isomer shift and quadrupole splitting given in the following references by Darby Dyar[55] and Oh, et al.[56] B_4C, B_6Si, and SiC are all over-reducing at X/N = 0.25, where the limits for redox control in a waste glass melter will be around $0.05 < Fe^{2+}/Fe_T < 0.33$.[57–59]

3.5 | Summary of reductant effectiveness

Table 6 provides a summary of the properties and behaviors examined for the melter feeds with the selected reductant additives. Sucrose at C/N = 0.75, and coke and VB_2 at X/N = 0.25 have similar foaming statistics when added to the AP-106 melter feed when the numbers are presented in Table 6; however, the notable low-temperature foaming event with sucrose, shown in Figures 3 and 4, is absent from the feeds with coke and VB_2. Both coke and VB_2 also have the advantage of reducing acetonitrile evolution significantly. The redox state remains similar to that of sucrose in the final glass and SO_2 is retained as far as these experiments are concerned.

The other three reductants, B_4C, B_6Si, and SiC, are all more effective in peak foam suppression and they do not

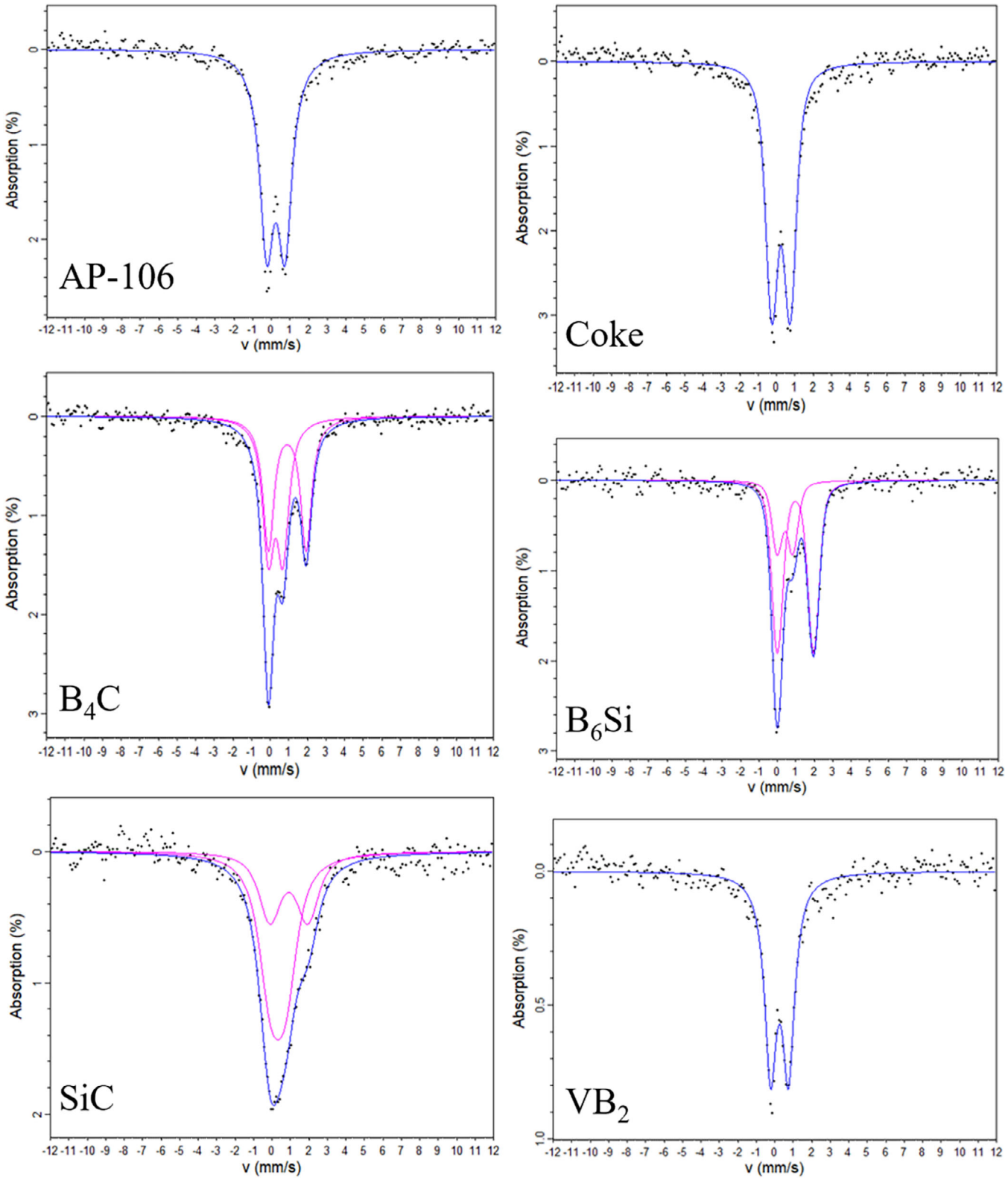

FIGURE 9 ^{57}Fe Mössbauer spectra of samples of AP-106 melter feeds batched with sucrose, coke, B_4C, B_6Si, SiC, and VB_2, and melted at 1150°C.

TABLE 6 A summary of properties of AP-106 melter feed with carbon-based and refractory-like ceramic reductants explored in this study.

Reductant additive	X/N ratio (X = C, Si, V)	Peak normalized foam volume (V/V_o)	Peak foam temperature (°C)	Total acetonitrile released (mg)	Fe^{2+}/Fe_T
Sucrose	0.75	21.1	775	150.80	<0.10
Coke	0.25	22.5	769	0.053	<0.10
B_4C	0.25	5.17	672	0.128	0.50
B_6Si	0.25	4.41	975	0.209	0.72
SiC	0.25	7.04	699	0.220	0.53
VB_2	0.25	19.5	690	0.040	<0.10

experience low-temperature foaming events. Of these, the feed with SiC is the one that most resembles an optimum foaming condition in Figure 6, as the foam peaks and collapses at a relatively low temperature, meaning it is less likely to be trapped beneath a more viscous glass-forming melt in a melter. Also absent from the table is the notable rapid release of gas in the feed with B_4C. The redox states of these, however, are outside of the contract limit $Fe^{2+}/Fe_T < 0.33$.[57–59]

4 | CONCLUSION

Alternative reductants to sucrose were tested in the simulated AP-106 hot commissioning melter feed. Refractory-like ceramics were selected on the basis that they are thermally stable and could produce similar success in foam and redox control to BN in previous work.[18] Coke dust in various forms was selected based on both being thermally stable, well demonstrated in industrial glass melting and being a by-product of another industry. All the feeds with alternate reductants showed a considerable reduction in the off gassing of toxic acetonitrile compared to sucrose. They also showed no SO_2 evolution at bench scale, suggesting SO_3 is well retained in the glass. Results were mixed for control of foaming, and coke and VB_2 additives were similarly effective to sucrose in controlling foaming overall but without any signs of low-temperature foaming that was observed in the sucrose feed. B_4C, SiC and B_6Si all reduced both maximum foaming and the total foam volume across the temperature range, however the final glasses were over reduced. The results indicate that comparing the coke and VB_2 at X/N ratios of 0.25 to the sucrose at C/N = 0.75 is appropriate, but for the other reductants, a further reduction in this ratio may be required to get comparable results. The rapid release of gas from B_4C and coke at C/N = 0.75 elevated ratios will likely rule these out of further scaled-up melter testing, however testing is suggested as future work based on the present study for the other alternative reductants to determine viability for processing, and for the baseline AP-106 feed with sucrose to ensure that the low-temperature foaming is not going to be an issue in larger melters.

ACKNOWLEDGMENTS

The authors gratefully acknowledge financial support from the U.S. Department of Energy (DOE) Waste Treatment and Immobilization Plant Project. Pacific Northwest National Laboratory is operated by Battelle for DOE under contract DE-SAC05-76RL01830. The authors are thankful to Scott Brombosz and Ian Gray from Emerging Energy & Sustainability at Phillips 66 for providing coke samples and technical discussions around how they were generated.

REFERENCES

1. Marcial J, Riley BJ, Kruger AA, Lonergan CE, Vienna JD. Hanford low-activity waste vitrification: a review. J Hazard Mater. 2024;461:132437. https://doi.org/10.1016/j.jhazmat.2023.132437
2. Peterson RA, Buck EC, Chun J, Daniel RC, Herting DL, Ilton ES, et al. Review of the scientific understanding of radioactive waste at the U.S. DOE Hanford site. Environ Sci Technol. 2018;52(2):381–96. https://doi.org/10.1021/acs.est.7b04077
3. Colburn HA, Peterson RA. A history of Hanford tank waste, implications for waste treatment, and disposal. Environ Prog Sustainable Energy. 2020;40(1):e13567. https://doi.org/10.1002/ep.13567
4. Matlack KS, Muller IS, Pegg IL. Low activity waste tuning feed material testing final report, VSL-18R4350-1. The Catholic University of America, Vitreous State Laboratory, Washington, DC; 2018. https://doi.org/10.2172/1974460
5. Westesen AM, Carney AM, Alvarez C, Turner JE, Trang-Le TT, Peterson RA. Cesium removal from AP-106 tank waste using crystalline silicotitanate. PNNL-35919 Rev. 0. Pacific Northwest National Laboratory, Washington; 2024. https://doi.org/10.2172/2474984
6. Goel A, McCloy JS, Pokorny R, Kruger AA. Challenges with vitrification of Hanford high-level waste (HLW) to borosilicate glass—an overview. J Non-Cryst Solids: X. 2019;4:100033. https://doi.org/10.1016/j.nocx.2019.100033
7. Hrma P. Effect of heating rate on glass foaming: transition to bulk foam. J Non-Cryst Solids. 2009;355(4–5):257–63. https://doi.org/10.1016/j.jnoncrysol.2008.10.009

8. Kappel J, Conradt R, Scholze H. Foaming behavior in glass melts. Glastechnische Berichte-Glass Sci Technol. 1987;60(6):189–201.
9. Gerrard AH, Smith IH. Laboratory techniques for studying foam formation and stability in glass melting. Glastechnische Berichte. 1983;56K:13–18.
10. Hujova M, Pokorny R, Klouzek J, Lee SM, Traverso JJ, Schweiger MJ. Foaming during nuclear waste melter feeds conversion to glass: application of evolved gas analysis. Int J Appl Glass Sci. 2018;9(4):487–98. https://doi.org/10.1111/ijag.12385
11. Schweiger MJ, Hrma P, Humrickhouse CJ, Marcial J, Riley BJ, TeGrotenhuis NE. Cluster formation of silica particles in glass batches during melting. J Non-Cryst Solids. 2010;356(25–27):1359–67. https://doi.org/10.1016/j.jnoncrysol.2010.04.041
12. Pokorny R, Hrma P. Mathematical modeling of cold cap. J Nucl Mater. 2012;429(1–3):245–56. https://doi.org/10.1016/j.jnucmat.2012.06.020
13. Marcial J, Pokorný R, Kloužek J, Hrma P, Schweiger MJ, Goel A. Effect of water vapor and thermal history on nuclear waste feed conversion to glass. Int J Appl Glass Sci. 2021;12(2):145–57. https://doi.org/10.1111/ijag.15803
14. Pokorny R, Hilliard ZJ, Dixon DR, Schweiger MJ, Guillen DP, Kruger AA, et al. One-dimensional cold cap model for melters with bubblers. J Am Ceram Soc. 2015;98(10):3112–18. https://doi.org/10.1111/jace.13775
15. Pokorny R, Hrma P. Model for the conversion of nuclear waste melter feed to glass. J Nucl Mater. 2014;445(1):190–99. https://doi.org/10.1016/j.jnucmat.2013.11.009
16. Abboud AW, Guillen DP, Hrma P, Kruger AA, Klouzek J, Pokorny R. Heat transfer from glass melt to cold cap: computational fluid dynamics study of cavities beneath cold cap. Int J Appl Glass Sci. 2021;12(2):233–44. https://doi.org/10.1111/ijag.15863
17. Rigby JC, Dixon DR, Kloužek J, Pokorný R, Thompson PBJ, Scrimshire A, et al. Alternative reductants for foam control during vitrification of high-iron High level waste (HLW) feeds. J Non-Cryst Solids. 2023;608:122240. https://doi.org/10.1016/j.jnoncrysol.2023.122240
18. Taylor-Pashow K Choi AS, McClane DL, McCabe DJ. Iodine distribution during evaporation of Hanford waste treatment plant direct feed low activity waste effluent management facility simulant. Savannah River National Laboratory., South Carolina; 2019. https://doi.org/10.2172/1569638
19. Hrma P Schweiger MJ, Humrickhouse CJ, Moody A, Tate RM, Rainsdon TT, et al. Effect of glass-batch makeup on the melting process. Ceramics–Silikaty. 2010;54(3):193–211.
20. Bagwell CE, Asmussen RM. Biotic degradation of acetonitrile limitations, controls, and conversion rates (PNNL-29786). Pacific Northwest National Laboratory, Washington; 2020. https://doi.org/10.2172/1661194
21. Matlack K, Pegg I. Estimates of acetonitrile generation from scale melter testing of LAW simulants (VSL-19S4573-1, Rev A) (ORP-67600-00/VSL-19S4573-1). Vitreous State Laboratory, The Catholic University of America, Washington, DC; 2019. https://doi.org/10.2172/1844981
22. Ryan JL. Redox reactions and foaming in nuclear waste glass melting (PNL-10510). Pacific Northwest National Laboratory, Washington; 1995. https://doi.org/10.2172/108181
23. Choi AS. Melter off-gas flammability assessment for DWPF alternate reductant flowsheet options (SRNL-STI-2011-00321; p. SRNL-STI-2011-00321, 1019027). Savannah River National Laboratory, South Carolina; 2011. https://doi.org/10.2172/1019027
24. Choi A. DWPF melter off-gas flammability model for the nitric-glycolic acid flowsheet (SRNL-STI-2014-00355). Savannah River National Laboratory, South Carolina; 2014. https://doi.org/10.2172/1154717
25. Rigby JC, Marcial J, Pokorny R, Kloužek J, Han KS, Washton N, et al. Boron nitride: novel ceramic reductant for low-activity waste vitrification. J Am Ceram Soc. 2025;108:e20192. https://doi.org/10.1111/jace.20192
26. Vernerova M Klouzek J Nemec L. Reaction of soda-lime-silica glass melt with water vapour at melting temperatures. J Non Cryst Solids. 2015;416:21–30. https://doi.org/10.1016/j.jnoncrysol.2015.02.020
27. Hubert M, Faber AJ, Sesigur H, Akmaz F, Kahl S-R, Alejandro E, et al. Impact of redox in industrial glass melting and importance of redox control. In Sundaram SK (Ed.), Ceramic engineering and science proceedings (pp. 113–28). Hoboken: John Wiley & Sons, Inc; 2017. https://doi.org/10.1002/9781119417507.ch11
28. Adamec J, Levitin LY, Litvin VI, Tokarev VD, Yachevskii AV. Rational approaches to regulating the redox properties of batch for float-glass production. Glass Ceram. 2012;68(9–10):273–81. https://doi.org/10.1007/s10717-012-9370-z
29. Fedorov AG, Pilon L. Glass foams: formation, transport properties, and heat, mass, and radiation transfer. J Non-Cryst Solids. 2002;311:154–73. https://doi.org/10.1016/S0022-3093(02)01376-5
30. Suopajärvi H, Salo A, Paananen T, Mattila R, Fabritius T. Recycling of coking plant residues in a Finnish steelworks—Laboratory study and replacement. Resources. 2013;2(2):58–72. https://doi.org/10.3390/resources2020058
31. Kuasoski M, Doliveira SLD, Silva A, Q., Panhoca L, Shevchenko I. Recycling of powder coke to cost-effective adsorbent material and its application for tertiary treatment of coking wastewater. J Cleaner Prod. 2020;265:121765. https://doi.org/10.1016/j.jclepro.2020.121765
32. Katarzyna K, Le CH, Lauda P, Michal S, Bacalova T, Tadeusz P, et al. The fabrication of geopolymer foam composites incorporating coke dust waste. Processes. 2020;8(9):1052. https://doi.org/10.3390/pr8091052
33. Toda A, Yamamura R, Taguchi K, Fukushima T, Kaji H. Kinetics of "melting" of sucrose crystals. Cryst Growth Des. 2018;18(4):2602–8. https://doi.org/10.1021/acs.cgd.8b00234
34. Beckett ST, Francesconi MG, Geary PM, Mackenzie G, Maulny APE. DSC study of sucrose melting. Carbohydr Res. 2006;341(15):2591–99. https://doi.org/10.1016/j.carres.2006.07.004
35. Solozhenko VL, Turkevich VZ, Holzapfel WB. Refined phase diagram of boron nitride. J Phys Chem B. 1999;103(15):2903–5. https://doi.org/10.1021/jp984682c
36. Graystar GNP. (n.d.). Thermal properties of ceramics. https://gnpgraystar.com/wp-content/uploads/2020/05/ThermalPropertiesofCeramicsPrintable.pdf. Accessed 1 Apr 2025.
37. Daviau K, Lee KKM. Decomposition of silicon carbide at high pressures and temperatures. Phys Rev B. 2017;96(17):174102. https://doi.org/10.1103/PhysRevB.96.174102

38. Crouch IG, Naebe M. The science of armour materials. 1st ed. Woodhead Publishing, Duxford, United Kingdom; 2017.
39. Solozhenko VL, Kurakevych OO. Melting and decomposition of orthorhombic B_6Si under high pressure. High Pressure Res. 2020;40(4):488–94 https://doi.org/10.48550/arXiv.2008.02739
40. Yuan Z, Xiong M, Yu D. A novel metallic silicon hexaboride, Cmca-B_6Si. Phys Lett A. 2018;384(126075):767–71. https://doi.org/10.1016/j.physleta.2019.126075
41. Wang P, Kumar R, Sankaran EM, Qi X, Zhang X, Popov D, et al. Vanadium diboride (VB_2) synthesized at high pressure: elastic, mechanical, electronic, and magnetic properties and thermal stability. Inorg Chem. 2018;53(3):1096–105. https://doi.org/10.1021/acs.inorgchem.7b02550
42. Salvador S, Commandre JM, Stanmore BR. Reaction rates for the oxidation of highly sulphurised petroleum cokes: the influence of thermogravimetric conditions and some coke properties☆. Fuel. 2003;82(6):715–20.
43. Ren B, Wang G, Zuo H, Xue Q, She X, Wang J. Reforming of converter gas with coke oven gas for thermochemical energy storage and carbon dioxide emission reduction. Fuel Process Technol. 2021;222:106957.
44. Contescu CI, Azad S, Miller D, Lance MJ, Baker FS, Burchell TD. Practical aspects for characterizing air oxidation of graphite. J Nucl Mater. 2008;381(1–2):15–24.
45. Wagnon T, Kirch N, Gallaher B. Repurposing Hanford waste tank AP-106 for interim storage of treated low-activity waste – 20044. WM Symposia, Inc, Tempe, AZ; 2020. https://www.osti.gov/biblio/23027932
46. Dixon DR, Stewart CM, Venarsky JJ, Peterson JA, Hall GB, Levitskaia TG, et al. Vitrification of Hanford tank waste 241-AP-107 in a continuous laboratory-scale melter. Pacific Northwest National Laboratory, Washington; 2019. https://www.osti.gov/biblio/1505629
47. Dixon DR, Westesen AM, Hall MA, Stewart CM, Lang JB, Cutforth DA, et al. Vitrification of Hanford tank 241-AP-107 with recycled condensate. Pacific Northwest National Laboratory, Washington; 2020. https://www.osti.gov/servlets/purl/1766813
48. Marcial J, Luksic S, Kloužek J, Vernerová M, Cutforth D, Varga T, et al. In-situ X-ray and visual observation of foam morphology and behavior at the batch-melt interface during melting of simulated waste glass. Ceram Int. 2022;48(6):7975–85. https://doi.org/10.1016/j.ceramint.2021.11.344
49. Ferkl P, Hrma P, Schweiger MJ, Pokorny R. Conversion kinetics during melting of simulated nuclear waste glass feeds. J Non-Cryst Solids. 2022;579:121363. https://doi.org/10.1016/j.jnoncrysol.2021.121363
50. Post-Guillen D. Bubbling behavior in a waste glass melter. 8th International Conference on Computational and Experimental Methods in Multiphase Flow, Valencia, Spain; 2015. https://www.osti.gov/servlets/purl/1360628
51. Pokorny R, Hrma P, Kruger AA. Mathematical modeling of cold cap: effect of bubbling on melting rate. Ceramics-Silikaty. 2014;58(4):296–302. https://www2.irsm.cas.cz/materialy/cs_content/2014/Pokorny_CS_2014_0000.pdf
52. Hilliard Z, Hrma P. A method for determining bulk density, material density, and porosity of melter feed during nuclear waste vitrification. J Am Ceram Soc. 2016;99(1):98–105. https://doi.org/10.1111/jace.13919
53. Matlack KS, Perez-Cardenas F, Pegg IL, Macedo PB, Buechele AC, Hojaji H, et al. Melter tests with LAW envelope A and C simulants to support enhanced sulfate incorporation (ORP-63503/VSL-01R3501-2). Vitreous State Laboratory, The Catholic University of America, Washington, DC; 2001.
54. Beerkens R. Redox and sulphur reactions in glass melting processes. Ceram Silik. 1999;43(3):123–31.
55. Darby Dyar M. A review of Mössbauer data on inorganic glasses: the effects of composition on iron valency and coordination. Am Mineral. 1985;70(3–4):304–16.
56. Oh SJ, Cook DC, Townsend HE. Characterization of iron oxides commonly formed as corrosion products on steel. Hyperfine Interact. 1998;112:59–66.
57. Jantzen C, Johnson F. Impacts of antifoam additions and argon bubbling on defense waste processing facility reduction/oxidation. Savannah River National Laboratory, South Carolina. 2012. https://doi.org/10.2172/1045616
58. Wicks GG, Heaton RC, Bibler NE. Redox chemistry in candidate glasses for nuclear waste. J Am Ceram Soc.1987;70(9):704–10. https://doi.org/10.1111/j.1151-2916.1987.tb05712.x
59. Schreiber HD, Schreiber CW, Riethmiller MW, Downey JS. The effect of temperature on the redox constraints for the processing of high-level nuclear waste into a glass waste form. MRS Proc. 1989;176:419. https://doi.org/10.1557/PROC-176-419

SUPPORTING INFORMATION

Additional supporting information can be found online in the Supporting Information section at the end of this article.

How to cite this article: Rigby J, Miller MG, Davidson S, Bohrmann NC, Marcial J, Seo J-H, et al. A comparison of ceramic and carbon-based reductants for vitrification of low-activity waste. Int J Appl Glass Sci. 2026;17:e70009. https://doi.org/10.1111/ijag.70009